DESIGNING PERMIAN BASIN FRACTURE TREATMENTS USING 3D FRACTURE SIMULATORS

Robert E. Barba, Jr.
Mark A. Linroth
Integrated Energy Services, Inc.

C. Ted Wooten
Meyer and Associates

Abstract

Three dimensional hydraulic fracture simulators have become increasingly popular in the Permian Basin. The choice of input parameters to these simulators can be critical to obtaining reasonable results. When sufficient effort is put forth to estimate these parameters, fracture height can be predicted prior to the job. This can be critical if water bearing zones are in close proximity to the hydrocarbon zones of interest. Field examples are discussed from the Delaware, San Andres, and Spraberry to demonstrate the value of proper parameter selection for 3D models in predicting fracture height.

Introduction

In a 1990 the Gas Research Institute conducted a survey on fracture design techniques. The survey found that the most widely used technique was the two-dimensional hydraulic fracture simulator (2D). The 2D models were used on 54% of the designs. The next most prevalent technique was no model on 31% of all designs. A distant third was the three dimensional fracture model (3D), accounting for only 15% of all designs.[1]

The 2D models assume a fixed hydraulic fracture height. In many cases, hydraulic fracture treatments do not stay confined within a fixed height, as the 2D models assume.[2,3] In the Permian Basin of West Texas the majority of the formations that are fracture stimulated do not have strong confining stresses.[4] This significantly limits the effectiveness of the 2D models. Three dimensional hydraulic fracturing simulators overcome this limitation of a fixed height by calculating the fracture height from treatment parameters and formation properties. The inputs required are considerably more involved, as the 3D models require rock properties from both the pay sands and boundary layers. Only 15% of the engineers surveyed in the GRI study indicated they felt they had sufficient knowledge and expertise to evaluate the created dimensions of a fracture using the 3D models. The objective of this paper is to describe a cost effective method of obtaining the required data, and give engineers a greater degree of comfort with 3D hydraulic fracture models.

3D Model Input Requirements

To obtain reasonable results from a 3D model, four main data subsets are required.[5] These four subsets are:

> **A. Permeability distribution**
> **B. Stress profile**
> **C. Other formation parameters**
> **D. Treatment parameters**

The first assumption in hydraulic fracture design is that the greater the accuracy of the input parameters, the more reasonable the numerical solution. Model results must be compared to actual field based results in order to validate this theory. A validation technique commonly utilized is to match model predicted treating pressures with actual field measurements.[6] This can be misleading, though, as the pressure solutions generated by 3-D fracture models are inherently non-unique. Therefore, the pressure matching technique must be supplemented with additional empirical data before fracture geometry can predicted with a high degree of confidence.

One method that can be utilized to supplement pressure matching is to run a 3D simulation on producing zones which have water nearby. If the subject well is known to be producing from a zone that has mobile water nearby (i.e., correlative offset wells were fracture stimulated with post-frac production generating high water cuts), the 3D model can be useful in evaluating treatment design options that could keep subsequent fractures from penetrating the known water zone(s). Characterizing the physical and mechanical properties using common well logs and using 3-D fracture geometry models to predict fracture geometry will be discussed in this paper. Well performance and fracturing pressure comparisons will be used to validate the methodology.

Development of the Permeability Thickness Profile

The first input parameter subset to evaluate is the permeability thickness profile. This has three main functions:

I. **Productivity profile** - How are the hydrocarbons distributed?

II. **Productivity estimate** - What effect will a frac treatment have on production?

III. **Fluid efficiency estimate** - How much fluid is actually creating the fracture?

The importance of permeability should be apparent from the above. The main issue to then address is the source of the data.

Permeability Sources

The preferred source of in-situ permeability and skin is a pressure transient test. This method of testing includes the analysis of the rate/pressure relationship during a stabilized production period or the more commonly used pressure buildup technique. There are many drawbacks to the pressure transient test, especially in low permeability reservoirs.[7] The second source is from log data calibrated to the results from the in-situ measurements.[8,9] This will be the most frequently used technique as logs are generally more available than pre-frac production tests. Core data corrected to in-situ conditions can be used as a fourth choice. The last source to use is a guess based on none of the above. Unfortunately, this is the most frequently used method in pre-frac formation evaluation.

The accuracy of the permeability thickness estimate is related to the type of reservoir and to the information that is available on the reservoir. Sandstone gas reservoirs are often the simplest to evaluate, followed by sandstone oil reservoirs. Both of these can be adequately characterized with well logs when test information is available.[8,9] Carbonate reservoirs can be characterized as well, however well tests are required more frequently due to the weak porosity-permeability relationships encountered. These three options will be discussed in more detail.

Log Derived Permeability and Net Pay

Much work has been done in the area of estimating permeability from logs.[10,11,12] Although the relationships between log measurements and reservoir physical properties such as permeability and hydrocarbon saturation must be established for each reservoir, logs can be useful in determining net pay and establishing a porosity cutoff for a given reservoir.

Bulk Volume Water Irreducible (BVW_{irr}) is a critical parameter in estimating net pay and productivity. The traditional method of obtaining BVW_{irr} is to observe water saturations in zones that produce no water, then multiply the water saturation by porosity. The zone from 8138 to 8173 in Fig. 1 is a good example of a zone that produces with a low water cut. The BVW in this zone is approximately 0.05 to 0.055, and an estimate of 0.05 for BVW_{irr} is therefore reasonable. If there are no low water cut zones in an area, there are guidelines presented in Table 1.

The first concept of log derived permeability is that the higher the effective porosity is above the value of BVW_{irr} for a given zone, the higher the effective hydrocarbon permeability. If porosity is less than or equal to BVW_{irr}, effective hydrocarbon permeability will be equal to zero. Fractured reservoirs provide exceptions to this, however an evaluation of this type of reservoir is beyond the scope of this study. The second concept as it relates to net pay is that BVW values above BVW_{irr} suggest that some water production can be expected. The higher BVW is above BVW_{irr}, the higher the water production. The sand from 7928 to 7936 in Fig. 2 produces significant amounts of water when it has been tested. The BVW in this zone is as high as 0.10, suggesting water production if a BVW_{irr} of 0.05 is assumed.

These BVW_{irr} values above are only guidelines and should be used only if there are no water free producing zones to calibrate the BVW to production. In fining upward or coarsening upward sequences the BVW_{irr} should be varied to adjust for grain size differences. In these variable BVW_{irr} zones promising results have been obtained with Nuclear Magnetic Resonance (NMR) technology.[13] This technique estimates BVWirr and effective porosity directly from log data independent of resistivity and conventional porosity measurements.

Log Derived Permeability Option 1 - Sandstone Reservoirs

The relationship between porosity (Φ), BVW_{irr}, and effective hydrocarbon permeability (k_e) can be quantified if the proper inputs are available[8,9,14,15]. The basic relationship developed is:

$$k_e = (C * \Phi^2 * (\Phi_e - BVW_{irr})/BVW_{irr}))^2 \qquad (1)$$

where:

k_e = effective hydrocarbon permeability (md)
C = constant
Φ_e = effective porosity (V/V)
BVW_{irr} = Bulk Volume Water Irreducible (V/V)

An example of the output is presented as Fig. 3. The permeability thickness profile indicates the permeable intervals for use in the fracture design model and productivity estimates in the optimization process. The effective permeability to hydrocarbons is used for productivity estimation. This technique has been validated with accurate predictions of post-fracture well performance[8,9,13].

From the equation above, it can be seen that any porosity value less than BVW_{irr} would result in a negative permeability estimate. This is particularly valuable in zones where BVW_{irr} is known and a calibration permeability is not available. In this case the default "C" factor of 100 can be used to obtain an approximation of core permeability, and net pay can be estimated using a core permeability cutoff.[15] Several studies have been done that show the effects of stress on core permeability, and these can be used as a guideline.[16,17] Core permeabilities, effective to air, are often reduced by an order of magnitude for approximating in-situ permeabilities to hydrocarbons. Thus a 0.1 md log derived core permeability would be a reasonable estimate for a maximum of 0.01 md at in-situ conditions. This reduction is a function of both the initial permeability and confining stress.[16,17]

Log Derived Permeability Option 2 - Carbonate Reservoirs

Carbonate reservoirs often contain complex pore throat structures and secondary porosity, and construction of a reliable porosity-permeability relationship is not always straightforward. Work done by the Bureau of Economic Geology suggested that sonic porosity provided a stronger porosity-permeability relationship than neutron-density porosity in San Andres dolomites.[18] The following relationship was developed for carbonate reservoirs:

$$k_e = (C * \Phi_S^2 * (\Phi_S - BVW_{irr})/BVW_{irr}))^2 \quad (2)$$

where:

k_e = effective hydrocarbon permeability
C = constant
Φ_S = sonic log porosity
BVW_{irr} = Bulk Volume Water Irreducible

The guidelines for BVWirr presented in Table 1 can be used with the core based "C" of 100 to help estimate net pay, however quantitative estimation of permeability from logs is difficult. To estimate productivity prior to stimulation, the most economic method is to perform a transient pressure test with automated well sounding equipment or production test after the perforations have been cleaned up with acid. If only the production test is done an estimate of skin must be made based on past experience with completion techniques.

Log Derived Permeability Option 3 - Sandstone Gas Reservoirs

An additional advantage sandstone gas reservoirs have is the sizeable Gas Research Institute database acquired in the Staged Field Experiment. As part of the SFE a comprehensive study was conducted to estimate in-situ permeability to gas and water from porosity data. Over 2000 core plugs were analyzed under simulated in-situ conditions to develop a correlation that could be used in a permeability thickness profile.[19,20,21] The relationships developed in these studies are as follows:

$$K\,inf = 6.47E7 * \Phi_e{}^{\wedge 8.03} \quad \text{(clean sandstones)} \quad (3)$$

$$K\,inf = 3.52E4 * \Phi_e{}^{\wedge 5.81} \quad \text{(siltstones)} \quad (4)$$

$$K\,brine = 0.52 * Kinf^{\wedge 1.13} \quad (5)$$

$$K\,gas = K\,brine * [(0.97*\Phi_e - BVW)/(0.97*\Phi_e - BVWirr)]^{\wedge 1.13} \quad (6)$$

$$K\,water = K\,brine * [(BVW-BVWirr)/(\Phi_e - BVWirr)]^{\wedge 8.22} \quad (7)$$

where

K_{inf} = Klinkenberg (gas slippage) corrected permeability
Φ_e = Effective porosity
BVW_{irr}= Bulk Volume Water Irreducible

Permeability for Fracturing Fluid Leakoff Estimates

While permeability can be used to help estimate fluid efficiency, a minifrac treatment is recommended to quantify the fracturing fluid leak-off behavior even if in-situ reservoir permeability from a well test is available.[22,23,24] In addition to the physical differences between reservoir and fracturing fluids, the permeability to fluids may be stress dependent. If this is the case, permeability may increase with increased fluid pressure.[25]

Development of the In-Situ Stress Profile

The in-situ stress profile is the second major input to the 3D model. It is one of the primary mechanical properties used to determine whether a treatment should be designed with a two dimensional or a three dimensional fracture simulator. In the case of the 3D simulator, it is the principal input used to estimate height growth.[26] As the well test is the calibration standard for permeability, the microfracture treatment or microfrac is the calibration standard for estimating the closure stress profile.[27] The microfrac involves injecting a small volume of fluid into perforations above fracturing pressure, and for small volumes closure pressure should be only slightly higher than the ISIP. The microfrac technique can be enhanced by employing high resolution crystal quartz pressure gauges with real time surface readout capability. Fig. 4 illustrates the mechanical setup for the test, while Fig. 5 illustrates a typical pressure response observed during a microfrac. Although the cost of these treatments has dropped considerably with increased competition in the quartz gauge market, the cost is still in the $12,000 to $15,000 range for a one day test.[28] A more economic method was needed to estimate the fracture gradient distribution from logs on each well.

A number of studies have addressed the estimation of this critical parameter from openhole wireline data. A reasonable match between log derived and measured values has been obtained in tectonically relaxed areas such as the Permian Basin and East Texas.[29,30] The most widely used relationship for log derived stress is:

$$F.G. = v/(1-v) * OBG + (1-(v/1-v)) * Pp + Ptec \qquad (8)$$

where:

$F.G.$ = Fracture gradient (psi/ft)
v = Poisson's Ratio
P_p = Pore pressure gradient (psi/ft)
P_{tec} = Tectonic offset
OBG =Overburden stress gradient (psi/ft)

The variables in this model will be discussed in detail.

Poisson's Ratio (v)

Poisson's ratio is a critical input to the elastic model. It basically relates the amount of vertical overburden that is transformed into horizontal stress assuming an elastic medium. The most direct source is from a full wave sonic measurement where a shear and compressional travel time has been obtained.[29] The relationship is:

$$\nu = [((\Delta t_S/\Delta t_C)^2-2]/[2*(\Delta t_S/\Delta t_C)^2-1] \qquad (9)$$

where

Δt_S = Delta T Shear (microseconds/ft)
Δt_C = Delta T Compressional (microseconds/ft)

There have been several hundred full wave sonic logs run in the Permian Basin by one service company alone, and most of the wireline service companies have tools that can measure both shear and compressional travel time. A more in-depth discussion of the applications of the full wave sonic technology can be found in refs 4, 9, 14, 20, 31, and 32. Even with the widespread availability of the technology, there may not be data available for the well that is to be stimulated. If there is a full wave sonic suite available on a correlative well, a reasonable correlation can often be made to the new well. Fig. 6 shows a flow chart that can be used to perform this correlation. The correlation requires an estimate of lithology to be made for each zone in both the offset well and the target well. There is a strong relationship between lithology and Poisson's ratio, and the Poisson's estimate from the full wave sonic well can be correlated via this method.

As a quality control technique, the values for Poisson's ratio should fall within a normal range that is dependent upon lithology. The range for these values can be seen in Table 2. Full wave sonic data quality can be affected by hole conditions or processing problems, and occasionally bad data will be encountered. These values can be used with care in areas where no data are available. As Table 2 should demonstrate, the variability within lithologies makes this technique a second choice to having measured values.

Pore Pressure Gradient

The pore pressure or reservoir pressure gradient is another critical input to the model. In an ideal situation it should be measured by either a wireline formation tester or a transient pressure test. In many cases, though, all that will be available will be a gradient from an offset well test somewhere in the field. The effect of pore pressure can be seen by varying it in Eq. 8 and holding the other variables constant. In typical San Andres dolomite, a 1000 psi reduction in reservoir pressure would result in a fracture closure pressure reduction of 600 psi. For a Grayburg siltstone at the same depth, a 1000 psi drop in reservoir pressure would result in a 718 psi reduction in fracture closure pressure. The impermeable barrier rock should retain the original pore pressure regardless of any changes in reservoir pressure in the permeable reservoir rock. In reservoirs with weak barriers this suggests that the zones could be drawn down prior to stimulation, with greater pressure drawdowns resulting in increased in-situ stress contrast.

In practical terms this increase in frac containment would be somewhat offset by the disadvantages of a slower post-frac cleanup and possible retention of fluid by undersaturated rock. If the zone requires stimulation to produce and there is water nearby, there may be no other option to reducing the reservoir pressure.

The concept of depletion warrants some further discussion for Permian Basin reservoirs. In many areas the virgin reservoir pressure gradient approaches the salt water gradient of 0.465 psi/ft. This is not always the case in the Permian Basin. The initial reservoir pressure in many fields is often less than the 0.465 gradient. In the Spraberry trend, the initial reservoir pressure in 1951 was never higher than 0.34 psi/ft.[33] Many other reservoirs have initial reservoir pressures less than the normal salt water gradient.[34] The best fit with field results has been obtained when the impermeable boundary layers are assigned the original field pore pressure gradient. This may not be the case in the majority of service company generated fracture height prediction logs, as it is common practice to use a constant pore pressure gradient in all layers. Extensive experience with these logs indicates the field net pressures routinely exceed the service company predicted net pressures to remain in zone, yet the 3D model, net pressure profile, and production results indicate better confinement.

Overburden Gradient

The third component of the log derived fracture gradient relationship is the overburden gradient. It is obtained directly from the bulk density measurement, with all of the available values averaged from the top of the pay zone to the surface. In practice the density log is only available up to the casing point, and only neutron and gamma ray data are available from casing point to surface. The overburden measurement should apply over a fairly broad area, and shallower offset wells can be used to extrapolate density data within a field. If not, geological input can be used to estimate lithology behind pipe, and the cased hole neutron porosity can be used to back out a bulk density measurement. Early references suggested that a gradient of 1.0 would be a good approximation if no other data were available.[4,14,29,30] Measured bulk density data in the Permian Basin suggests that gradients as high as 1.1 may be appropriate.[21] In all cases, the relationship to use in estimating overburden gradient is:

$$OBG = (\rho_b/1.1) * 0.465 \qquad (10)$$

where

OBG = Overburden stress gradient psi/ft
ρ_b = Bulk density g/cc

Young's Modulus

From the full wave sonic data and bulk density data, an estimate of Young's modulus can be made as well. The relationship used to develop a dynamic field Young's modulus is:[29]

$$E_{log} = 2 * G * (1+v) \quad (11)$$
$$G = (1.34*10^{10}) \times (\rho_b/\Delta TS^2) \quad (12)$$

where:

E_{log} = Dynamic Young's modulus (psi) from logs
G = Shear modulus (psi)
ρ_b = Bulk density

3D models require a static Young's modulus, while the log provides a dynamic measurement. The conversion of dynamic to static can be accomplished two ways. The method chosen depends upon the availability of laboratory data.

Young's Modulus Conversion Method A - Laboratory Data Available

If a full core is available it is recommended that a triaxial static Young's modulus be obtained from a representative sample. The laboratory can also estimate a dynamic Young's modulus using sonic data. The two values should be compared to develop a ratio of (laboratory static/laboratory dynamic) values. This multiplier should be less than one, with a range from 0.5 to 1 in most cases. This multiplier can be applied to the field dynamic estimate from the logs to obtain a field static estimate.[35]

Young's Modulus Conversion Option B - No laboratory data available

The results of several laboratory studies were compiled by the Gas Research Institute.[36] Excerpts from this study are presented as Figs. 7 and 8. The ratio observed was from 0.5 to 1, with the output a function of the absolute value of Young's modulus and the in-situ stress. In general the lower the dynamic Young's modulus and the lower the stress, the lower the multiplier is. The value of 50% can be used as a lower bound for any estimation. The GRI data was all collected in tight gas sands, and no laboratory data have been published for carbonate systems. Pressure matching done in this study in San Andres dolomites suggests a ratio of 0.25 may be appropriate for a dynamic to static conversion factor in that lithology.

Extrapolation of Young's Modulus to Offset Wells

Options A and B above assumed there was full wave sonic data available on the wells to be stimulated. As with Poisson's ratio discussed earlier, an extrapolation to a well without this data may need to be done. If a plot is made of porosity vs dynamic Young's modulus from available full wave sonic log data, it can be seen that a reasonable relationship exists. To better understand this, refer to Eqs. 11 and 12 above. The three key inputs are Poisson's ratio, shear travel time, and bulk density. Poisson's ratio is directly related to lithology, and the other two variables are directly related to porosity. An equation can be derived from the crossplot of dynamic Young's modulus and porosity for a given lithology. This dynamic Young's modulus estimate can then be reduced accordingly using Option A or B above. An example can be seen in Fig. 8.

Fracture Toughness

This parameter is measure of a material's resistance to fracture propagation, and is sometimes referred to as the critical stress intensity factor. Fracture toughness is an input that is usually not measured, and there has been no recent research done with any published data for specific lithologies. Van Eekelen (1982) summarized several earlier laboratory studies, and provided a range of values for various lithologies.[37] These values can be used if no other data are available, and they are presented in Table 3. They were used in the four field examples in this paper, and they were found to be reasonable if not somewhat high. The 25% dynamic to static Young's modulus conversion in dolomites discussed previously may have masked a lower fracture toughness value than the 950 psi in^.5 input for the example. The GRI SFE 3 well was used for a comparison of all commercially available fracture models, and a constant fracture toughness value of 2000 psi/in$^{0.5}$ was used in all layers.[38]

Fluid Loss Parameters

Numerical fracture geometry models generally use some form of leak-off coefficient (C_t) to account for the fluid lost to the formation during a fracture treatment.[22] This C_t is defined for modeling purposes to be in units of distance per unit time. This is convenient because when C_t is multiplied by the fracture area, the resultant is the volume loss per unit time. It is important to note that this leak-off coefficient is determined as a function of the particular fracture geometry model being used.

By definition C_t is comprised of three different mechanisms that control leak off behavior [23]

$$C_t = f(C_\mu, C_c, C_w) \quad where:$$

C_μ = leak-off viscosity coefficient
Cc = reservoir compressibility and viscosity coefficient
Cw = filter cake coefficient

In many low permeability fracturing applications the dominant factor that controls fluid leakoff is the nature of the filter cake deposited by the fracturing fluid on the fracture face during injection. This filter cake coefficient (C_w), although strongly coupled in reality, is independent of formation permeability for modeling purposes.

The time required for a fracture to close (i.e., lose all of the fluid stored in the fracture to the reservoir) can be related directly to the fluid efficiency. Fluid efficiency is a unitless parameter defined as the amount of fluid stored in the fracture at the end of injection, divided by the total amount of fluid injected into the formation during the fracturing treatment. With the use of numerical algorithms, the fluid efficiency can be related to the total leak-off coefficient (C_t). As was discussed previously, the preferred source of this C_t value is a minifracture treatment. The pressure decline following the minifracture treatment is monitored, and the Ct is a function of the estimated formation parameters fracture and the observed fracture closure time.

Treatment Parameters

The estimation of treatment parameters is perhaps the most straightforward in the 3D modeling process. Unlike the petrophysical and reservoir parameters discussed earlier, this area is one the fracturing service companies traditionally have the most experience. Attention should be paid to the actual fluids that are being pumped vs what was designed, as changes in fluid viscosity can have a major effect on 3D fracture geometry. On-site monitoring of fluid viscosities and break times should be done to verify that the input parameters are correct. Crosslinked fluids have received most of the attention in the literature, however many operators pump linear fluids or polyemulsions. Regardless of the fluid type pumped, accurate rheological indices need to be used if 3D modeling is to be done effectively. The effect of sand on linear fluid viscosity is much more significant than with crosslinked systems, and this needs to be incorporated into the modeling process to obtain reasonable matches with field pressures. Shah (1991) presented correlations for n prime and k prime that have helped obtain better matches.[40] The effects are not well documented for oil-water emulsion systems, however field experience suggests the viscosity increase with sand is greater than the linear gels. With the advent of portable PC technology, changes can be made to the design onsite if there are changes in the base fluid rheology. A minifracture treatment can be conducted the same day as the main treatment, and changes can be made to the schedule if fluid efficiency is different from the original assumptions.

Field Example I - Dawson Co. Upper Spraberry Sand with Water Zones Above

The main pay is an oil sand with a low resistivity water zone above. When the wells are successfully fracture treated 100-200 BOPD initial rates can be obtained in the high permeability area of the field. Four offset wells in this high permeability area have fractured into the water sands above with less than optimum results. A comparison of the initial producing rates for this high permeability area is shown as Fig. 9.

Well A was treated with 60,000 gal of 40 lb XLG and 120,000 lb of 20/40 Ottowa down the annulus between 5 1/2 inch casing and 2 3/8 inch tubing. The tubing pressure was monitored during the job to ensure that the treating pressure did not exceed the delta pressure prescribed by the full wave sonic based mechanical properties log. It tested initially for 180 BOPD and 30 BWPD and produced over 60,000 BO in the first year of production. There were four other offset wells in this high permeability sand completed in a similar manner, with excellent results on all four. A comparison of initial production results for the five successful completions and the four unsuccessful completions can also be seen in Fig. 9.

Log analysis was done on well A to confirm the presence of the water sand that was responsible for the poor performance of the four offsets. Fig. 10 shows the high porosity oil sand at 8150 and the water bearing sand at 7950. The 3D model was used to reconstruct the treatment of well A to confirm the avoidance of water. The log derived values of permeability and stress were input as per the procedures discussed in this paper. Fig 11 shows the in-situ stress profile used. The actual treatment schedule was input, and a comparison was made to the observed treating pressures. Fig. 12 shows the comparison between the dead string derived bottomhole frac pressure and the estimated bottomhole frac pressure from the 3D model. The 3D model predicted the fracture would grow predominantly down away from the water, and that the dead string pressures would increase approximately 130 psi during the job following initial extension. The actual job pressures increased 128 psi following extension. The 3D model (Fig. 13) predicted the top of the created fracture to be at 8030 and the top of the propped fracture to be at 8055, or 100 feet below the water zone.

Two interesting items can be gleaned from this field example. The first is that fracture height can be contained in an environment with relatively weak in-situ stress contrasts. Some fracture designers routinely use a radial model based on the assumption that there are no barriers, and this radial model would be clearly inappropriate in this case. The other item is the reasonable match with bottomhole measured pressures in the absence of any external factors such as roughness, tip effects, or fracture toughness values in excess of Table 3's estimates. These techniques are also used by some designers along with the radial model to explain the lack of a net pressure decline during height growth.

Field Example II - Andrews Co. San Andres Carbonate with Water Below

The well was in an area where similar problems had been encountered with water production, this time from below the pay zone. Two correlative offset wells had been completed on the lease prior to this well, and the average initial production from the two wells was 81 BOPD and 229 BWPD. Both had been completed down casing with 40,000 gal of crosslinked gel carrying 89,000 lb of 20/40. The objective of the new wells' completion was to adequately stimulate the oil zone while minimizing water production. The entire oil zone and the top of the water zones can be seen in Fig. 14. The main pay is from 4448 to 4478, while the moveable water starts at 4535. A higher permeability water zone is deeper than the log total depth at approximately 4600. Fig. 15 shows the in-situ stress profile used for the 3D design. A lower rate treatment was designed to keep the net pressure below the prescribed net pressure from the full wave sonic mechanical properties log. (Fig. 16). The job was also designed to go down tubing with the annulus open to monitor bottomhole fracture pressure. 30,000 gal of 30 lb crosslinked gel was pumped with 48,000 lb of sand prior to the pressure reaching its maximum allowable limit. The 3D model initially predicted a flat profile, while the actual dead string pressures suggested better containment. When the dynamic Young's modulus in the dolomite was decreased by a factor of 75% instead of 50%, the pressure match was excellent. A comparison of the dead string bottomhole frac pressure and the 3D model predicted bottomhole frac pressure can be seen in Fig. 17. The predicted fracture geometry can be seen in Fig. 18, with the base of the propped fracture at 4550. The production comparison in Fig. 19 suggests that the fracture avoided the high permeability 4600 ft. water zone below.

This example further discredits the radial fracture theory. In some cases the radial theory with excessive proppant settling may be used to explain avoidance of water zones above the productive zones. This could be argued in the previous case study, although the pressure match would probably not have been consistent with this conclusion. In this field example, though, the avoidance of water below presents strong support for the 3D geometry over the radial geometry.

Field Example III - Eddy County Brushy Canyon Sandstone with Water Above

The well is in an active area of the Delaware Basin where a variety of completion techniques have been employed to avoid water production. The Delaware sands are notorious for having weak fracture barriers and high permeability water sands surrounding the productive oil sands. The 3D model was run to help determine why some treatments were successful in avoiding water while others were not. The in-situ stress profile was dominated by the massive Bone Springs limestone immediately below the Brushy Canyon, with fairly weak siltstones above the oil pay. The 3D model suggested that the water sands would be penetrated by most treatments, but that the proppant may or may not remain across the water zones above depending upon the viscosity of the fluid used to carry the proppant. Several operators had reported better results with linear gel sand stages following crosslinked pads, and the 3D analysis indicated this type of schedule would result in less proppant across the water bearing zones above. This well was treated with 75,000 gal of 30 lb crosslinked gel and 271,075 lb of sand, and the initial production results suggested the water sands were propped with the all-crosslinked schedule. Figs. 20 through 25 show the log analysis, stress distribution, 3D model prediction, tracer survey, and surface treating pressure comparison for the well. The well was treated down casing and a bottomhole pressure measurement was not available. The log analysis, pressures, 3D geometry, tracer survey, and production results are in agreement.

Field Example IV - San Andres Carbonate Design Optimized with Minifracture Treatment

The well was a refracture candidate in an established field with significant pressure depletion expected. It had been on production for 15 years, and the operator felt that production could be improved by re-stimulating with a larger frac. Production was averaging 18 BOPD and 20 BWPD and the reservoir pressure was estimated to be approximately 650 psi at the time of the re-stimulation. A minifracture treatment was done prior to the frac with a downhole pressure bomb. This treatment provided a good estimate of both fracture closure pressure and total leakoff coefficient, and the main job was designed using this information.

The well was fracture treated with 16,500 gal of 30 lb borate XLG and 54,000 lb of 12/20 Ottowa. The calculated net pressure plot suggested excellent confinement with a tip screenout at the end of the job. The zone was a relatively high porosity dolomite with no water nearby (Fig 26), and the 15 years of production provided a fairly large reservoir pressure and in-situ stress contrast (Fig. 27). The 3D model parameters were selected in accordance with the guidelines discussed previously, and these were supplemented with the minifrac data. The permeability was varied to get a match with the minifrac pressure decline and the total fluid loss coefficient. The result was an excellent agreement between the 3D model predicted and actual surface treating pressures (Fig 28). The 3D geometry suggested that excellent confinement had been obtained (Fig. 29). The post frac production results were satisfactory as well, with the production increasing to 35 BOPD from 18 BOPD. This example also supports the premise that fractures can be contained, along with providing an excellent example of the confining effects of depletion.

Conclusions

1. 3D fracture models improve fracture geometry estimates when the reservoir physical and mechanical properties are accurately defined.

2. Improved openhole log interpretation and minifrac analysis provide economic methods for obtaining accurate reservoir descriptions to use in 3D modeling.

3. Successfully avoiding fracturing into known water bearing zones is shown to be an additional validation tool for fracture geometry models. When used in conjunction with the technique of matching measured treating pressures with model calculated pressures, operators can predict well future performance as related to proposed fracture treatment designs.

4. Accurate reservoir characterization can reduce the need to arbitrarily modify the mechanisms in fracture geometry models that affect the model calculated pressures. Documented numerical techniques for predicting fracture propagation pressures, friction pressure gradients, and proppant transport phenomenon are shown to be successful in predicting the final propped fracture geometry.

References

1. Holditch, S.A. and Associates: "Hydraulic Fracture Treatment Design and Implementation-Benefits of Applying New Technology," Seminar sponsored by the Gas Research Institute, 1992.
2. Cleary, M.P.: "Primary Factors Governing Hydraulic Fractures in Heterogeneous Stratified Formations," paper ASME 78-Pet-47 1978
3. Cleary, M.P.: "Mechanisms and Procedures for Producing Favourable Shapes of Hydraulic Fractures," paper SPE 9260, 1980b
4. Barba, R.E. : "Improving Return on Hydraulic Fracture Treatment Investment with Wireline Inputs," presented at the 33rd Annual Southwestern Petroleum Short Course, Lubbock, Tx. Apr 23-24 1986 p 57.
5. Meyer, B.R.: "MFRAC-II Hydraulic Fracturing Simulator Version 7.0 User's Guide," Meyer and Associates, Natrona Heights, Pa. November 1993.
6. Crockett, A.R., Willis, R.M.: "Improvement of Hydraulic Fracture Predictions by Real-Time History Matching on Observed Pressures," paper SPE 15264, 1987
7. Raghavan, R., Meng H-Z., and Reynolds, A.C. Jr.: "Analysis of Pressure Buildup Data Following a Short flow Period," JPT (April 1982) 904-916.
8. Barba, R.E. , Chaney, J., and Darling, H.: "Recent Advances in Log-Derived Permeability," presented at the 1990 Schlumberger Gulf Coast Interpretation Symposium, March 1990.
9. Barba, R.E. and Cutia, A.S.: "Evaluating Horizontal Well Potential in the Spraberry Trend," SPE paper 23949 presented at the 1992 Permian Basin Oil and Gas Recovery Conference, Midland, March 18-20.
10. Carman, P.C.:"Fluid Flow Through Granular Beds," Trans. Inst. of Chemical Engr 15, (1937) 150-166.

11. Timur, A.:"An Investigation of Permeability, Porosity, and Residual Water Saturation Relationships," Trans. SPWLA 9th Annual Logging Symposium, New Orleans June 26, 1968 paper K.
12. Coates, G.R. and Dumanoir, J.L.:"A New Approach to Log Derived Permeability," Trans SPWLA 14th Annual Logging Symposium, Lafayette, May 6-9 1973.
13. Miller, M.N.et al: "Spin Echo Magnetic Resonance Logging: Porosity and Free Fluid Index Determination," SPE paper 20561 presented at the 65th Annual Technical Conference and Exhibition, New Orleans, La. Sept. 23-26, 1990.
14. Barba, R.E. and Meyer, B.R.:"Integrating Wireline Data with Three-Dimensional Hydraulic Fracture Simulators in the Spraberry Trend," paper SPE 25509 presented at the 1993 SPE Production Operations Symposium, March 21-23, Oklahoma City.
15. Coates, G.R. and Denoo, S.: "The Producibility Answer Product," Schlumberger Technical Review, 29, No. 2 (June 1981), 55.
16. Thomas, R.D. and Ward, D.C.: "Effect of Overburden Pressure and Water Saturation on Gas Permeability of Tight Sandstone Cores," paper SPE 3634 presented at the 1971 SPE Annual Meeting, New Orleans.
17. Keelan, D.K.: "Automated Core Measurement System for Enhanced Core Data at Overburden Conditions," paper SPE 15185 presented at the 1986 SPE Rocky Mountain Regional Meeting, Billings, Mt. May 19-20.
18. Lucia, F.J. et al:"Calculation of Remaining Mobile Oil, Dune Field, University Lands, Crane County, Texas," presented at the 1988 Southwestern Petroleum Short Course, April 20-21, Lubbock, Tx. p.167.
19. Luffel, D. L., Howard, W.E., and Hunt, E.R.: "Relationships of Permeability, Porosity, and Overburden Stress Derived from an Extensive Core Analysis Database in the Travis Peak Formation," paper SPE 19008 presented at the 1989 Denver Low Permeability Reservoir Symposium.
20. Holditch, S.A., Whitehead, W.S., and Rahim, Z.;"Using In-Situ Stress and Permeability Thickness Profiles to Design the Well Completion," SPE paper 21493 presented at the 1991 Gas Technology Symposium, Houston Jan. 23-25.
21. Gas Research Institute, "Results of Applied Research in the Canyon Sands," workshop presented at the 1992 Permian Basin Oil and Gas Recovery Conference, Midland, Tx. March 18-20.
22. Meyer, B.R., "Design Formulae for 2-D and 3-D Vertical Hydraulic Fractures: Model Comarison and Parametric Studies", SPE 15240, 1986
23. Meyer, B.R., Hagel, M.W., "Simulated Mini-Frac Analysis", 39th Annual Technical Meeting of the Petroleum Society of CIM held in Calgary, June 1988
24. Nolte, K.G. and Economides, M.J.:"Pressure Analysis During Fracturing," Reservoir Stimulation, Schlumberger Educational Services, 1987 pp. 7-1 through 7-15.
25. Warpinski, N.R., Teufel, L.W., and Graf, D.C.:"Effect of Stress and Pressure on Gas Flow Through Natural Fractures," SPE paper 22666 presented at the 66th Annual Technical Conference and Exhibition, Dallas, Tx. Oct 6-9, 1991.
26 Warpinski, N.R., Schmidt, R.A., and Northrop, D.A.: "In-Situ Stresses - The Predominant Influence on Hydraulic Fracture Containment," SPE paper 8932, 1980.
27. Gas Research Institute: "Developing In-Situ Stress Profiles," GRI Technical Summary, Gas Research Institute, Chicago 1992.
28. Wood Group Production Technology, Inc., Houston, personal communication.

29. Newberry, B.M., Nelson, R.F., and Ahmed, U.: "Prediction of Vertical Hydraulic Fracture Migration Using Compressional and Shear Wave Slowness," paper SPE 13895 presented at the 1985 SPE/DOE Symposium on Low Permeability Reservoirs, Denver, May 19-22.
30. Whitehead, W.S., et al:"In-Situ Stresses: A Comparison Between Log Derived Values and Actual Field Measured Values in the Travis Peak of East Texas," SPE paper 15209 presented at the 1986 Unconventional Gas Technology Symposium, Louisville, Ky. May 18-21.
31. Barba, R.E.: "Improving Production in the Spraberry Trend With Wireline Inputs," presented at the 1987 Southwestern Petroleum Short Course, Lubbock, Tx. Apr 22-23 1987.
32. Barba, R.E. : "Optimizing Hydraulic Fracture Length in the Spraberry Trend," SPE Formation Evaluation, September 1989, p480.
33. Dyes, A.B. and Johnston, O.C.: "Spraberry Permeability from Buildup Analyses," Trans. AIME 1953, 198, pp 135-38.
34. Galloway, W.E. et al: "Atlas of Major Texas Oil Reservoirs," Bureau of Economic Geology, Austin, Tx. 1983, pp 83-85.
35. McLennan, J.D., personal communication.
36. Gas Research Institute, "Static vs. Dynamic Modulus," GRI Technical Summary, Gas Research Institute, Chicago 1992.
37. Van Eekelen, H.A.:"Hydraulic Fracture Geometry: Fracture Containment in Layered Formations," SPE paper 9261 presented at the 55th Annual Technical Conference and Exhibition, Dallas, Tx. Sept 21-24, 1980.
38. Warpinski, N.R., Moschovidis, Z.A., Parker, C.D., and Abou-Sayed, I.S.: "Comparison Study of Hydraulic Fracturing Models:Test Case - GRI-Staged Field Experiment No. 3," SPE Paper No. 25890 presented at the SPE Rocky Mountain Regional/Low Permeability Reservoirs Symposium, Denver, Colo. April 12-14, 1993.
39. Conway, M.W. and Penny, G.S., :"Hydraulic Fracturing," SPE Monograph Volume 12, Chapter 8.
40. Shah, S.N.: "Rheological Characterization of Hydraulic Fracturing Slurries," SPE paper 22839 presented at the 1991 Annual Technical Conference and Exhibition, Dallas, Tx. Oct 6-9.

Table 1 - Lithology vs. BVWirr

Lithology		**BVW_{irr}**
Coarse grained sands	:	**0.04-0.06**
Fine grained sands and silts	:	**0.06-0.10**
Limestones	:	**0.04**
Vugular dolomites	:	**0.02**
Sucrosic dolomites	:	**0.05-0.07**

Table 2 - Lithology vs. Poisson's Ratio

Lithology		Poisson's Ratio Range
Sandstones	:	0.15-0.20
Siltstones	:	0.20-0.26
Shales	:	0.26-0.30
Dolomites	:	0.28-0.30
Limestones	:	0.30-0.31
Anhydrites	:	0.31-0.32

Table 3 - Lithology vs. fracture toughness

Lithology	Fracture Toughness
Siltstone	1300 psi/in $^{1/2}$
Sandstone	1000 psi/in $^{1/2}$
Limestone	675 psi/in $^{1/2}$
Shale	750 psi/in $^{1/2}$

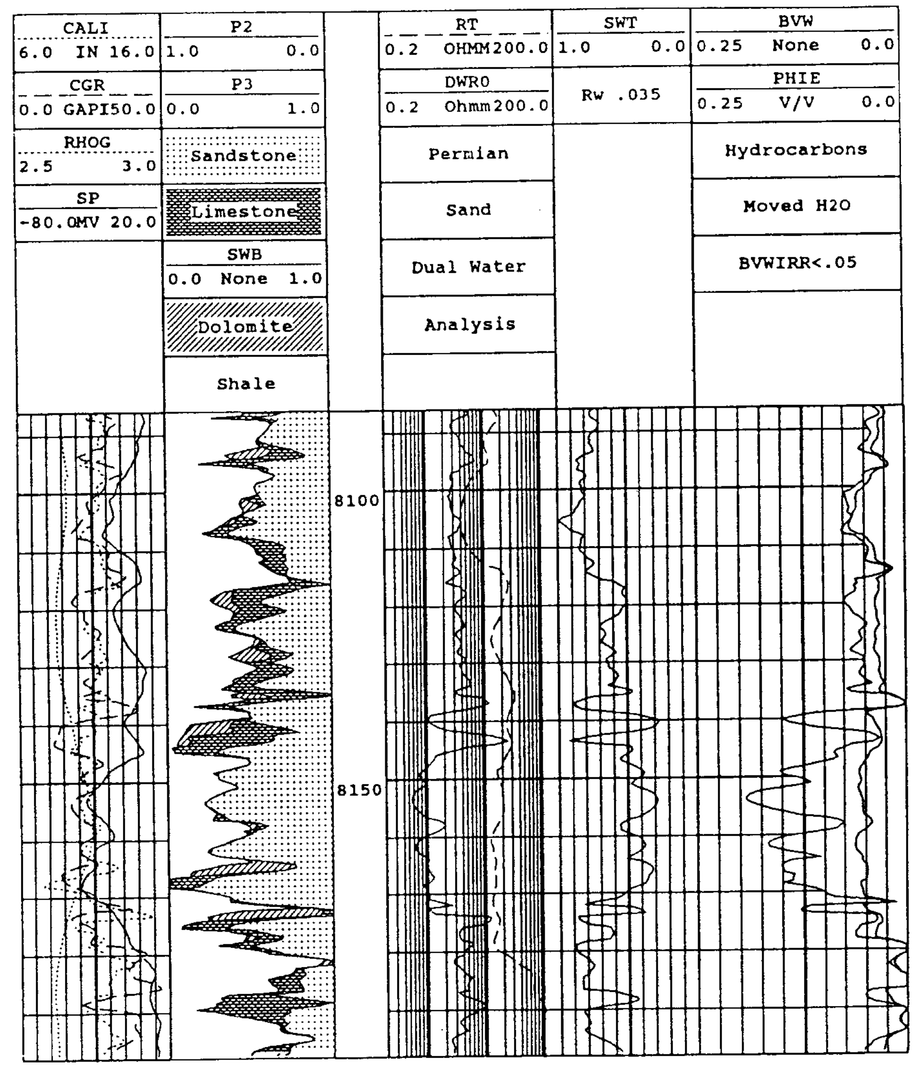

Figure 1

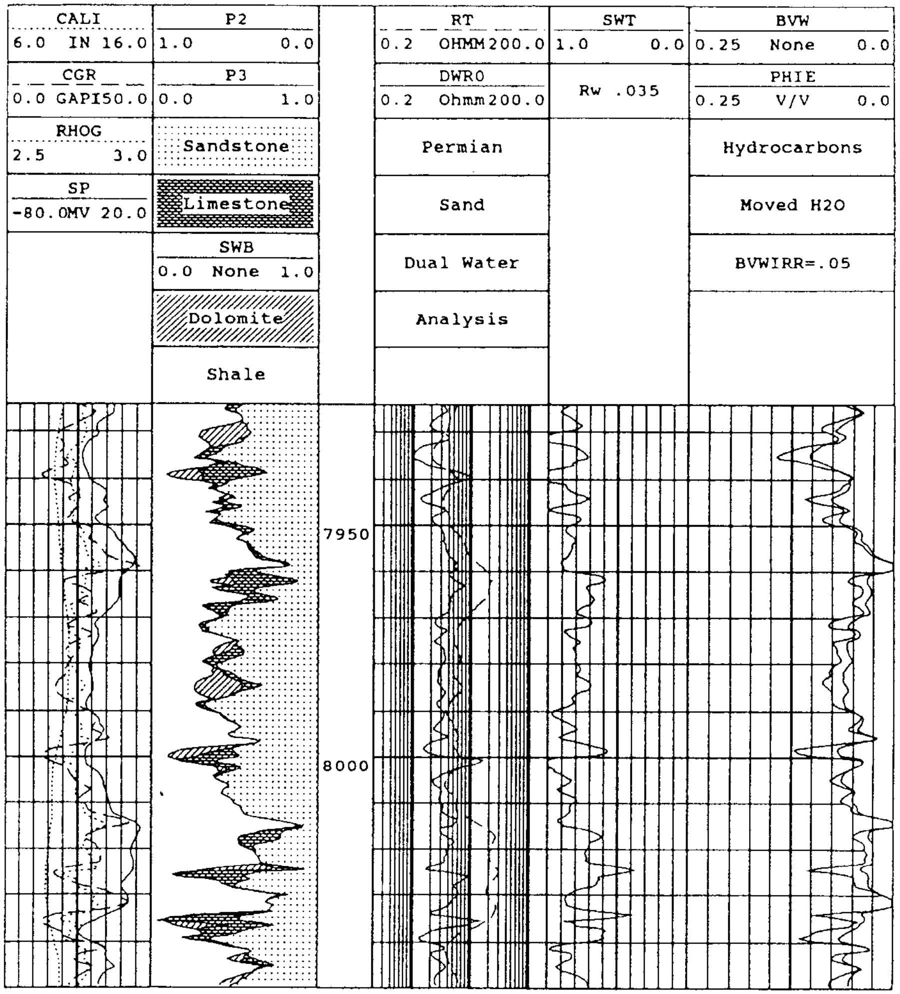

Figure 2

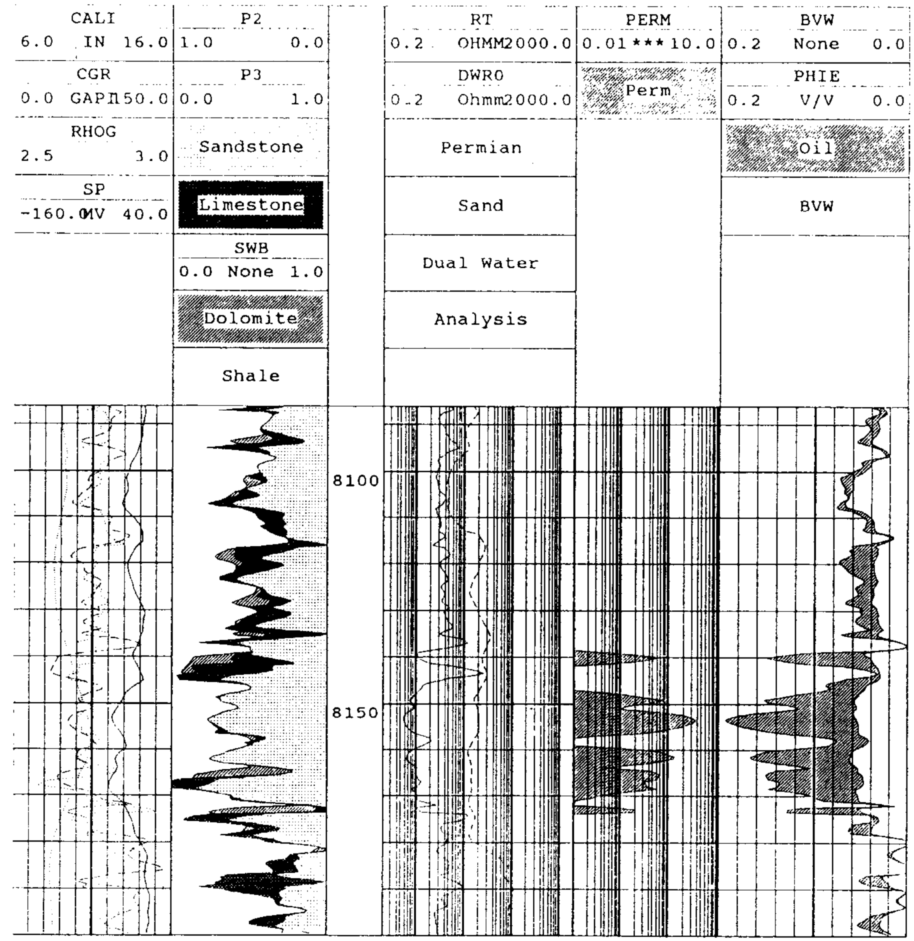

Figure 3

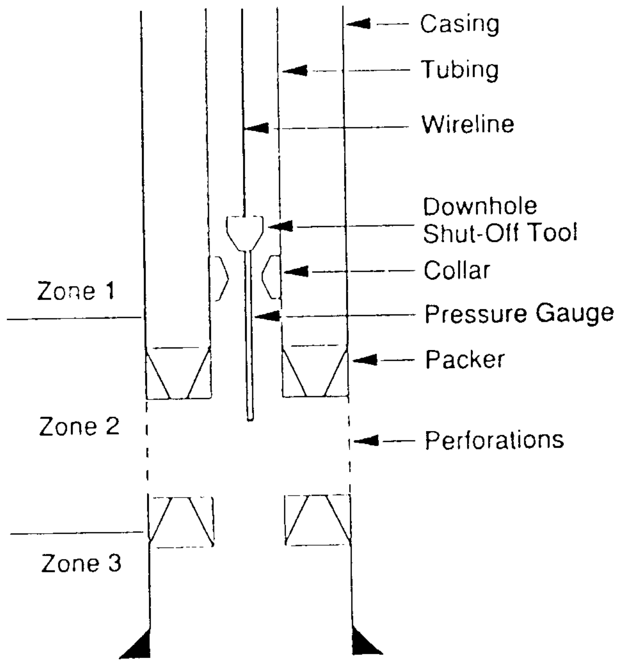

Figure 4 - Downhole in-situ stress measuring equipment

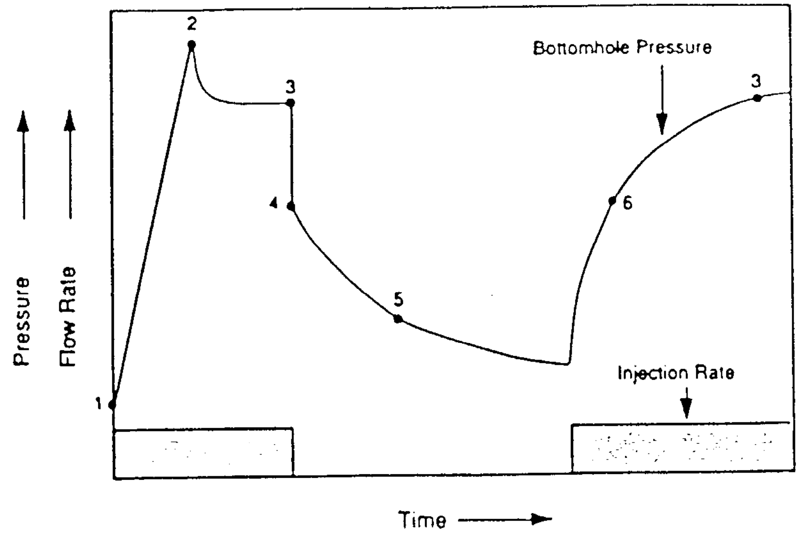

Typical pressure response observed in stress test

1. Hydrostatic pressure
2. Breakdown pressure
3. Fracture extension pressure
4. Initial shut-in pressure
5. Fracture closure pressure
6. Fracture reopening pressure

Figure 5

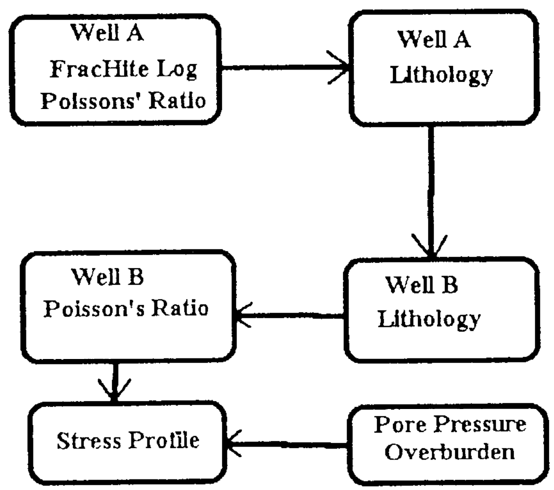

Figure 6 - Poisson's ratio correlation technique

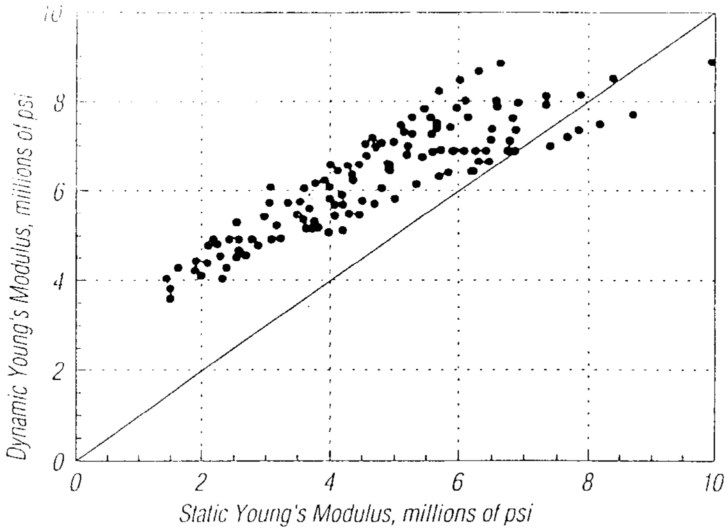

Comparison of static and dynamic Young's modulus; static values measured while axial load decreased[2]

Figure 7

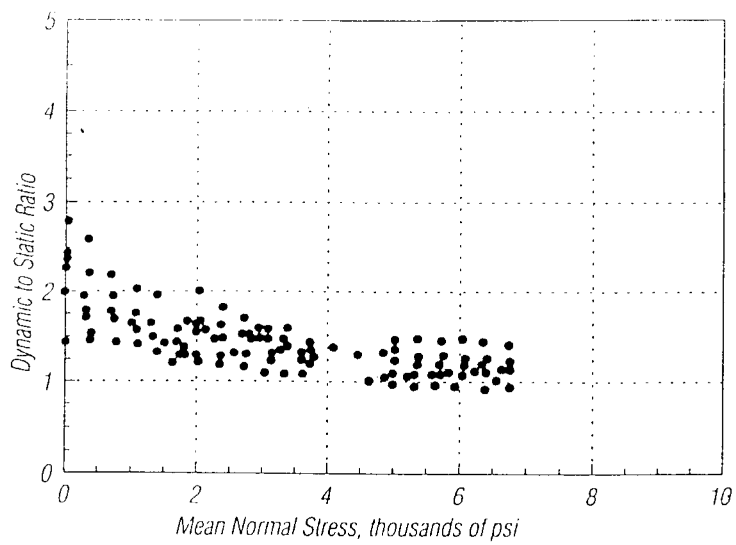

Ratio of dynamic to static Young's modulus as a function of mean normal stress[2]

Figure 8

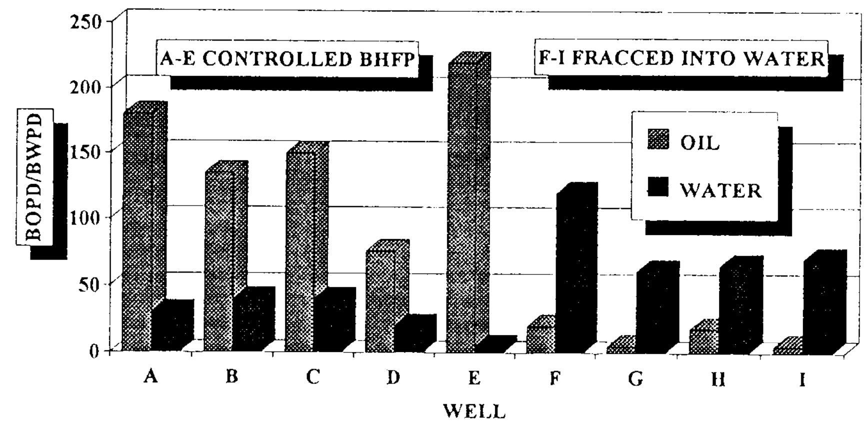

Figure 9 - Dawson Co. Upper Spraberry initial production rate distribution

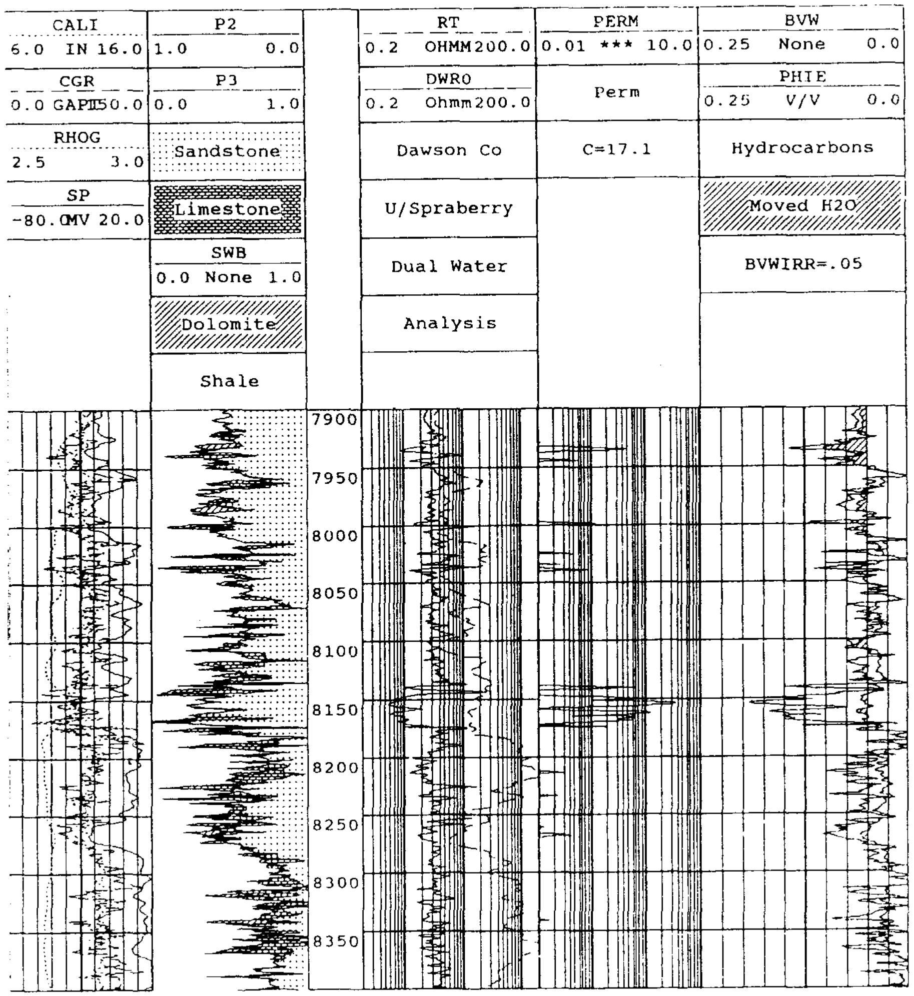

Figure 10

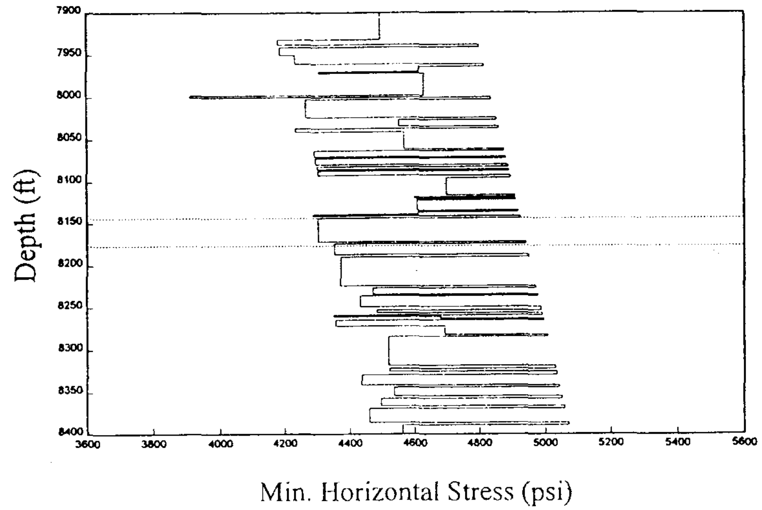

Figure 11 - Dawson Co. Upper Spraberry stren profile

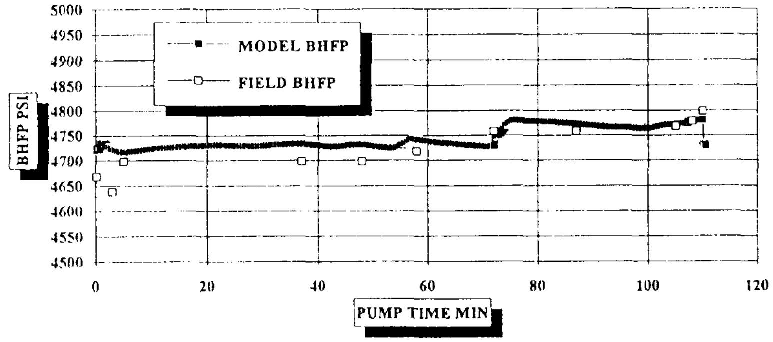

Figure 12 - Dawson Co. Upper Spraberry dead string bottomhole frac pressure vs. 3D model BHFP

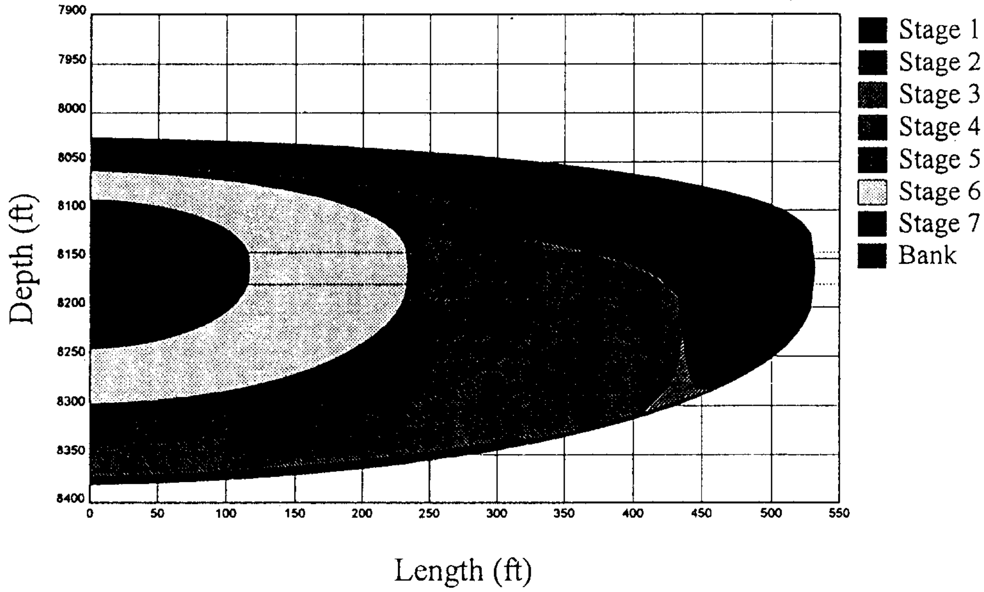

Figure 13 - Dawson Co. U/Spraberry proppant at closure (cluster)

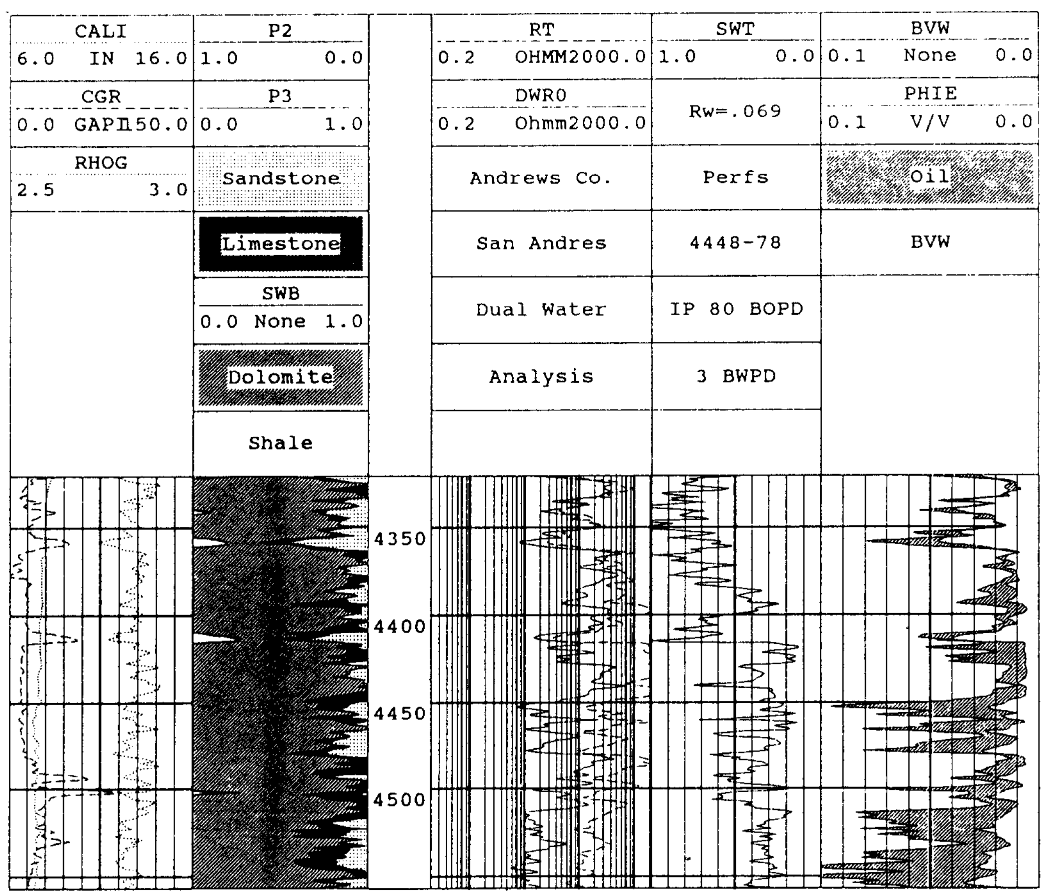

Figure 14

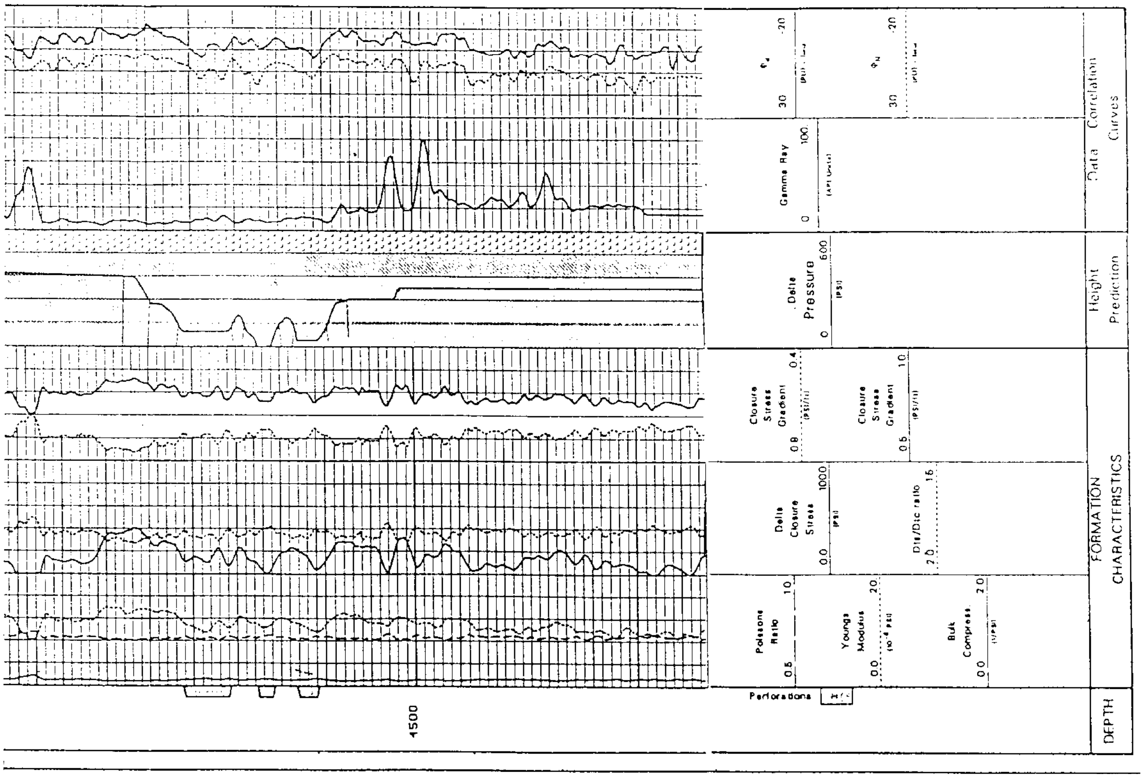

Figure 16

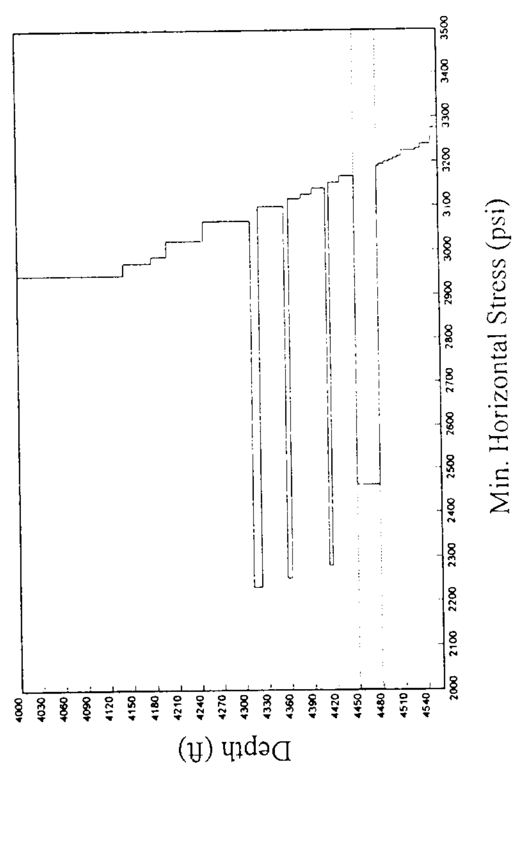

Figure 15 - Andrews Co. San Andres - Porosity Zones 0.2 PPG

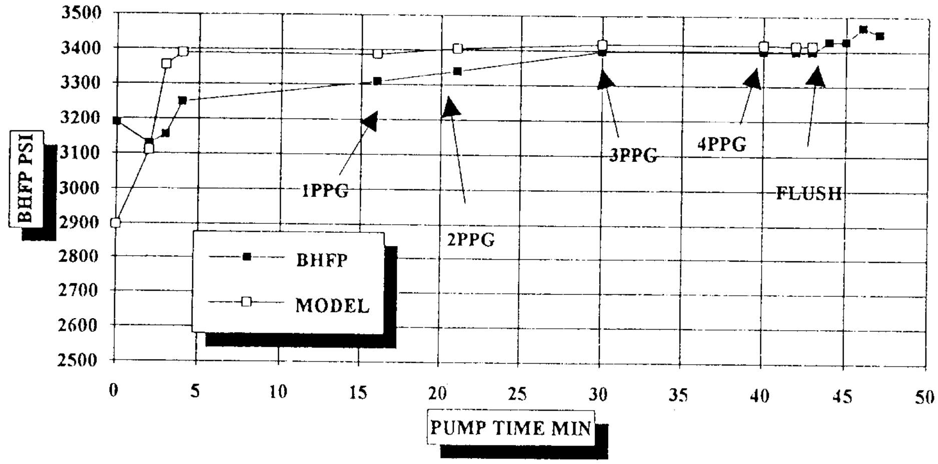

Figure 17 - Andres Co. San Andres bottomhole frac pressure comparison

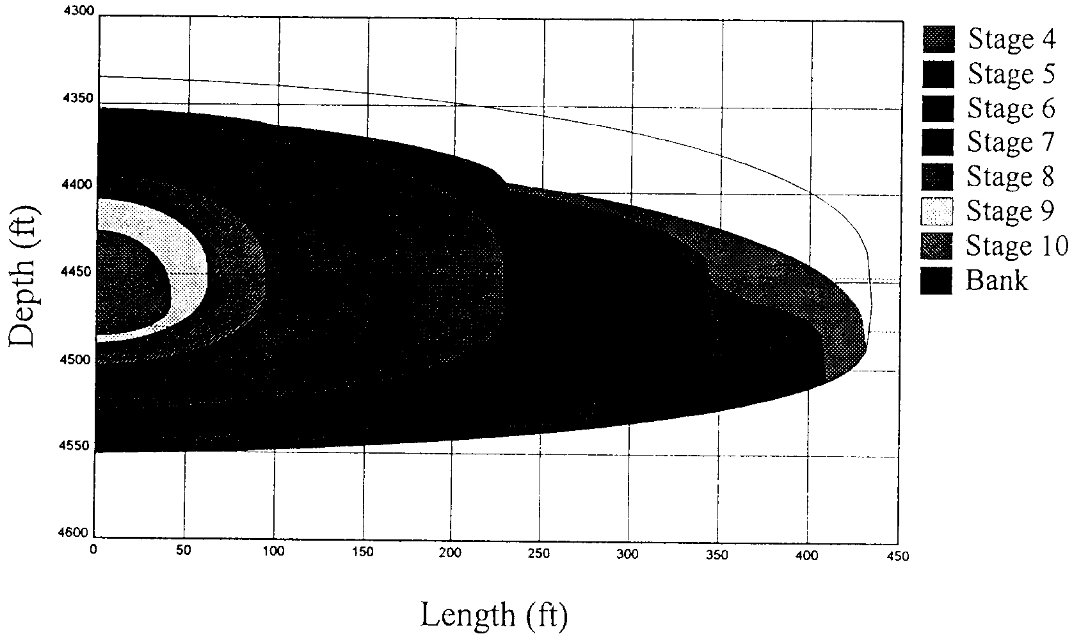

Figure 18 - Andrews Co. San Andres proppant distribution

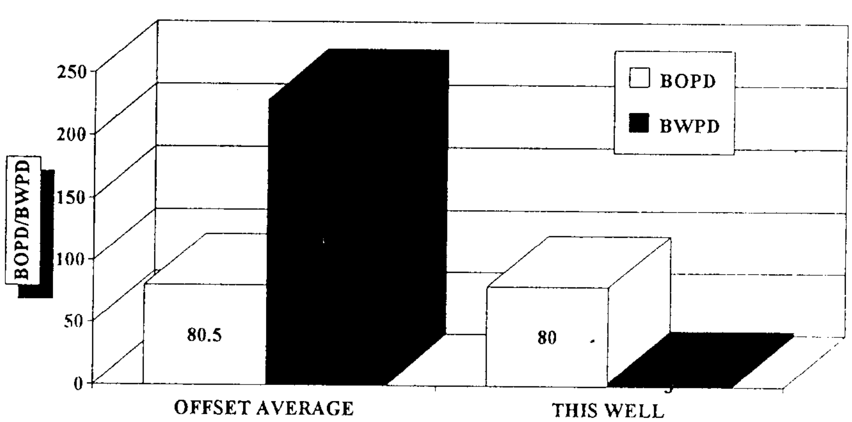

Figure 19 - Andrews Co. San Andres initial production comparison

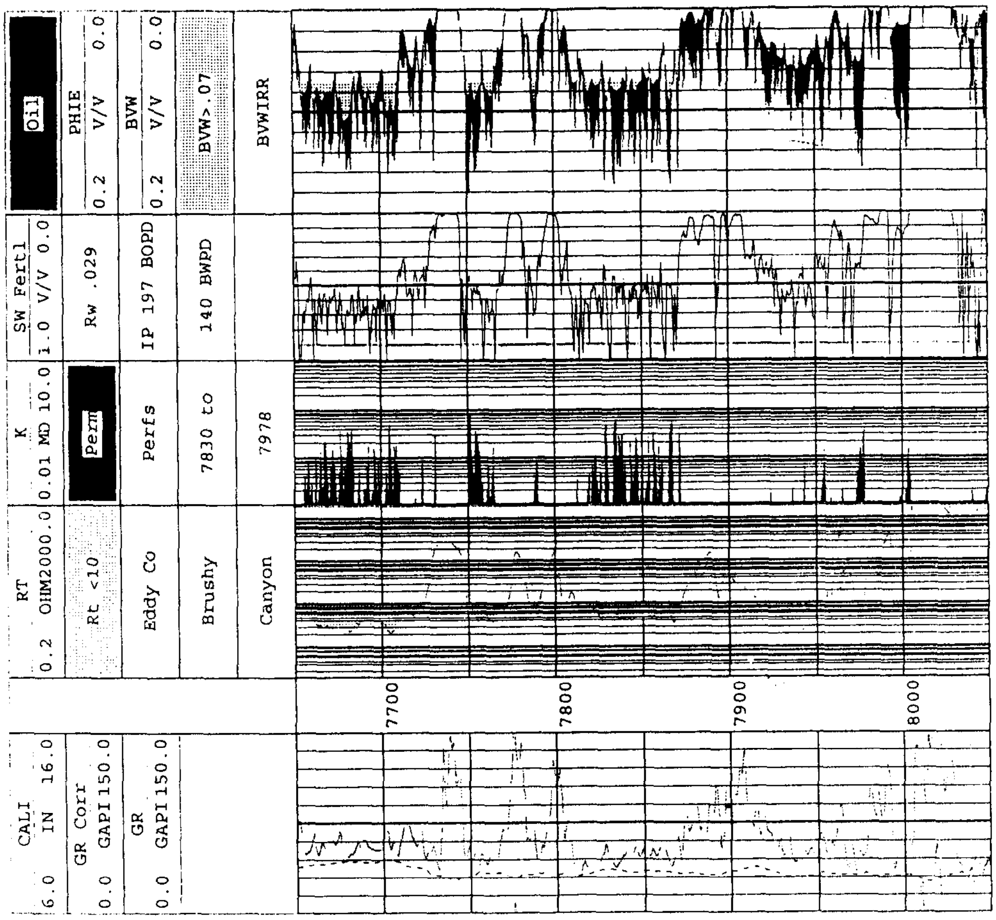

Figure 20

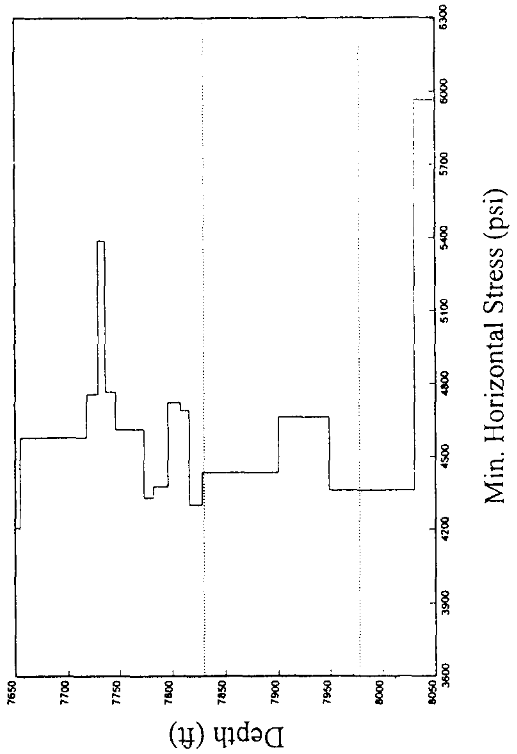

Figure 21 - Eddy Co. Brushy Canyon stress profile

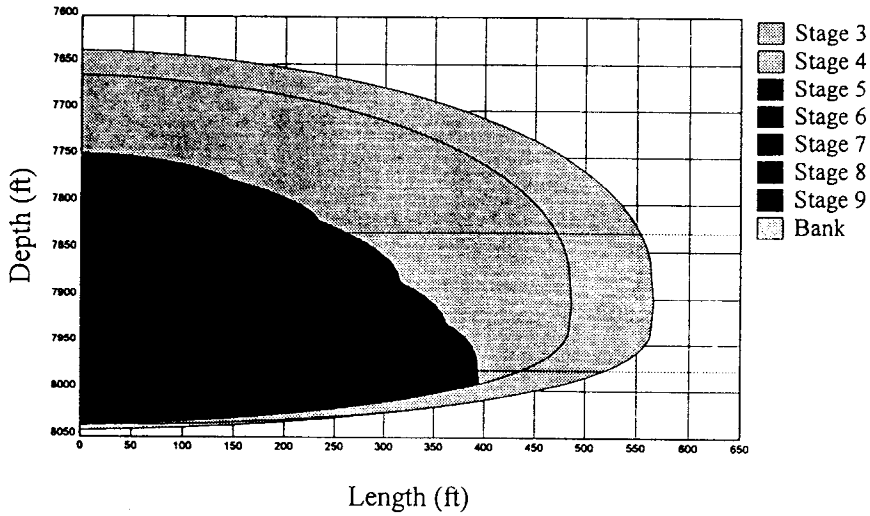

Figure 22 - Eddy Co. Brushy Canyon proppant distribution

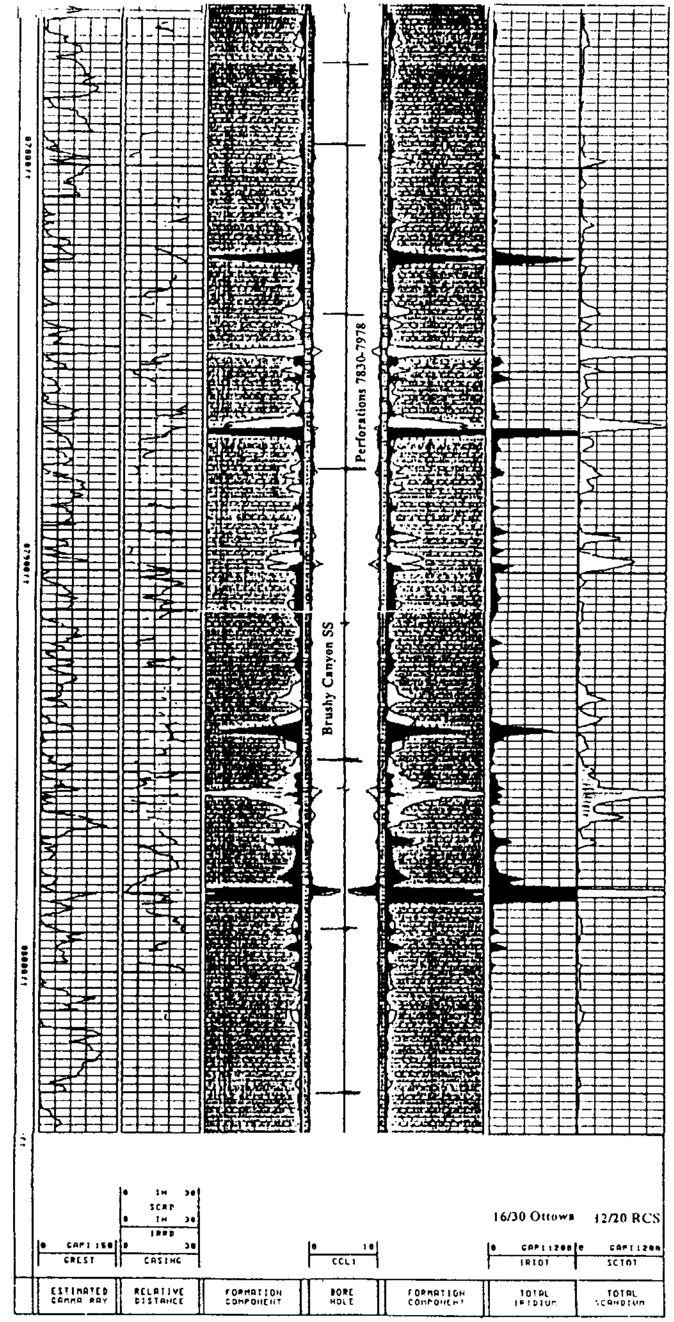

Figure 23

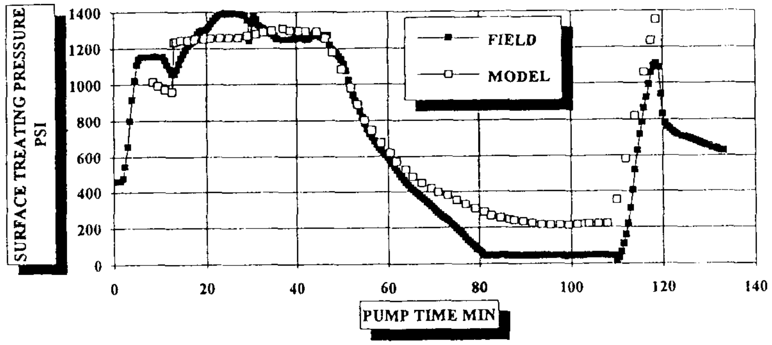

Figure 24 - Eddy Co. Brushy Canyon surface pressure comparison

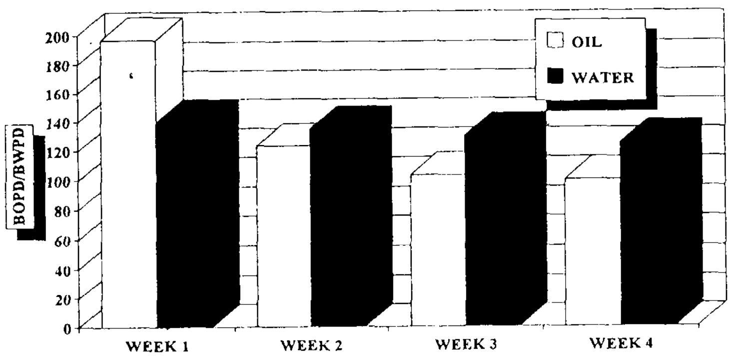

Figure 25 - Eddy Co. Brushy Canyon first month's production

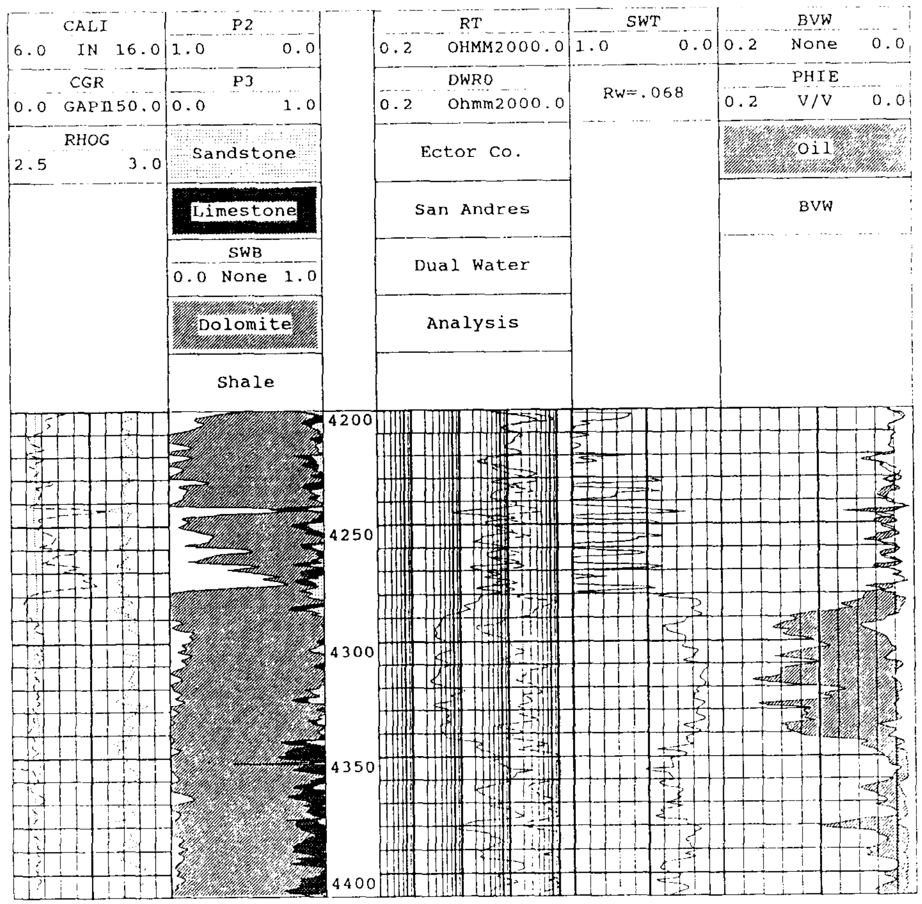

Figure 26

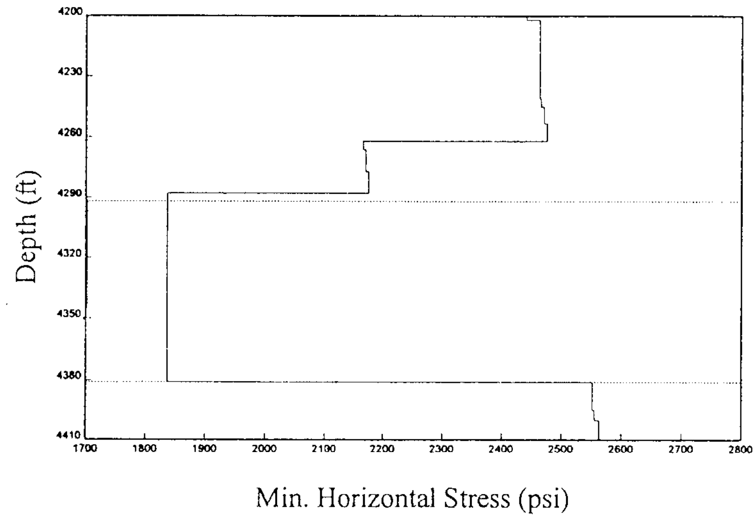

Figure 27 - Ector Co. San Andres stress profile with 0.15 PPG

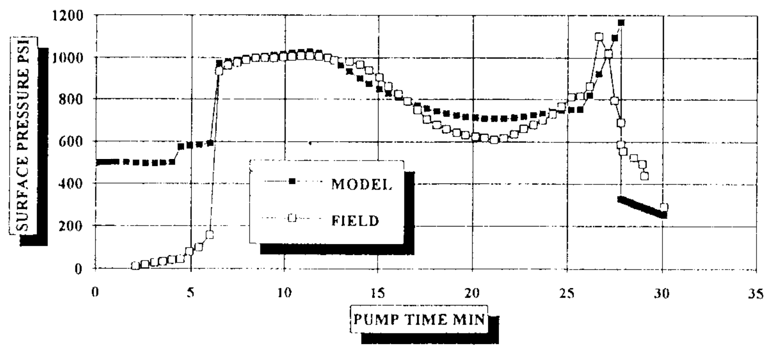

Figure 28 - Ector Co. San Andres surface treating pressure vs. 3D model prediction

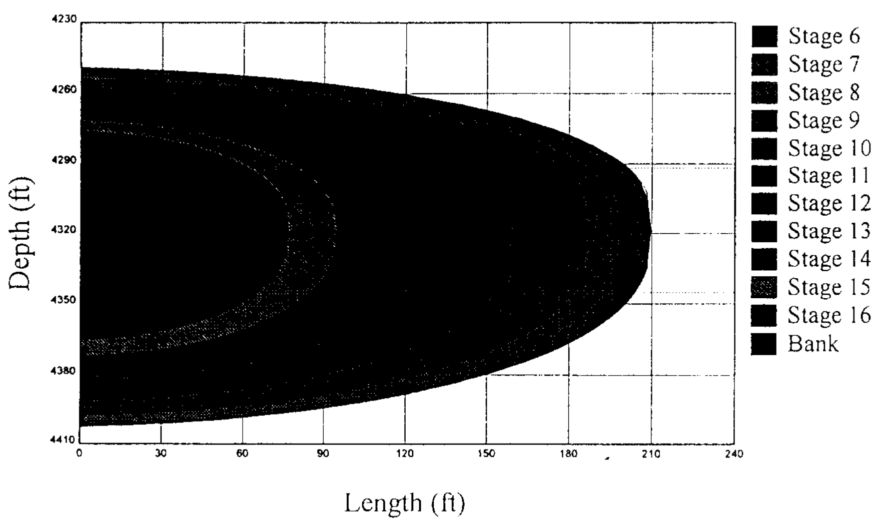

Figure 29 - Ector Co. San Andres proppant distribution